water

MDPI

Article

Water Quality Characteristics and Source Analysis of Pollutants in the Maotiao River Basin (SW China)

Yinjiu Li [1,2,3], Qiuhua Li [1,2,*], Shulin Jiao [3], Chen Liu [1,2], Liuying Yang [3], Guojia Huang [4], Si Zhou [5], Mengshu Han [2,6] and Anton Brancelj [2,7,8]

1 Key Laboratory for Information System of Mountainous Area and Protection of Ecological Environment of Guizhou Province, Guizhou Normal University, Guiyang 550001, China; liyinjiu123@163.com (Y.L.); 18679169725@163.com (C.L.)
2 Guizhou International Science & Technology Cooperation Base-International Joint Research Centre for Aquatic Ecology, Guizhou Normal University, Guiyang 550001, China; hanmengshu112@163.com (M.H.); Anton.Brancelj@nib.si (A.B.)
3 School of Geography and Environmental Science, Guizhou Normal University, Guiyang 550025, China; jiaoshulin@gznu.edu.cn (S.J.); liuyingyang1985@163.com (L.Y.)
4 School of Environment and Biological Engineering, Guiyang University, Guiyang 550005, China; huangguo.jia@163.com
5 Department of Aquatic Ecological and Environmental Research, Provincial Environmental Science Research and Design Institute, Guiyang 550002, China; zhousi2022@163.com
6 Key Laboratory for Information and Computing Science of Guizhou Province, Guizhou Normal University, Guiyang 550001, China
7 Department for Ecosystems and Organisms Research, National Institute of Biology, 1000 Ljubljana, Slovenia
8 Faculty of Environmental Sciences, University of Nova Gorica, 5000 Nova Gorica, Slovenia
* Correspondence: qiuhua2002@126.com

Abstract: Rivers are an important mediator between human activities and the natural environment. They provide multiple functions, including irrigation, transportation, food supply, recreation, and water supply. Therefore, evaluations of water quality and pollution sources are of great significance for ecological restoration and management of rivers. In this study, the improved "vušekriterijumska optimizacija i kompromisno rješenje" (VIKOR in Serbian; in English: Multicriteria Optimization and Compromise Solution), and a geodetector were used to analyze the water quality characteristics and pollution sources of the Maotiao River Basin (Gizhou province, SW China). The results showed that the water quality of the Maotiao River Basin deteriorated significantly during the summer drought period, as was evident in the reservoirs and lakes. It improved in the wet season (i.e., during the summer period) due to runoff dilution. Water quality decreased along the river's course, from upstream to downstream sections. The results of the geographic detector analysis showed that agricultural areas were the primary factor affecting the spatial distribution of water quality in the river basin. In July, August, and November 2020, the influence of agricultural land was 0.72, 0.60, or 0.80, respectively, and the interactions among urban, industrial, agricultural, and forested areas explained 99.2%, 83.2%, or 99.9% of the spatial differentiation of water quality, respectively. Due to the influence of spatial scale, settlements have a small influence on the spatial distribution of water quality. Their impact factors were 0.38, −0.24, and −0.05, respectively. Notably, the negative relationship of water quality and forested areas reflects that topography, types of landscapes, and soil thickness have considerable influences on the Maotiao River Basin's water quality. Based on the findings, we infer that good farmland water conservancy projects and comprehensive management of different types of landscapes, such as forests, agriculture, and urban area and water bodies, are of great significance for improving water quality.

Keywords: water quality; source analysis; improved multicriteria optimization and compromise solution; geodetectors

Citation: Li, Y.; Li, Q.; Jiao, S.; Liu, C.; Yang, L.; Huang, G.; Zhou, S.; Han, M.; Brancelj, A. Water Quality Characteristics and Source Analysis of Pollutants in the Maotiao River Basin (SW China). *Water* **2022**, *14*, 301. https://doi.org/10.3390/w14030301

Academic Editors: Rossella Albrizio, Anna Maria Stellacci, Vito Cantore and Mladen Todorovic

Received: 8 December 2021
Accepted: 10 January 2022
Published: 20 January 2022

1. Introduction

Since entering the Anthropocene, the impact of human activities on the global ecological environment has become increasingly prominent [1]. Unlike the shortage of water resources in the arid regions of Northwest China, structural water shortages in southern China are caused by water pollution, and have gradually become one of the most common problems faced by the Chinese society. Rivers are an important ecological and economical link between human society and the natural environment. Through their self-purification processes, rivers are efficient means of supplying water, both in terms of quality and quantity [2]. They play an important role in high-quality and intensive economic development. Therefore, effective and accurate assessing of river water quality (and quantity) is a necessary condition for the comprehensive management of different types of landscape: urban, agricultural, and forested, including the high-mountain regions [3–10]. Currently, there are two main principles that are adopted for river water quality evaluations. Both are based on DPSIR: Drivers, Pressures, Status, Impacts, Reactions [11]. The first principle uses biological sensitivity and biodiversity to assess the impact of human activities on rivers. However, this method focuses on a wide biological community structure and cannot reflect the complexity of the river's habitats, i.e., biotic and abiotic elements [12–14]. The second method involves the comprehensive index method, which integrates water quality, hydrology, river characteristics, biology, and types of landscapes through the construction of an evaluation index system, already incorporated in the European standards for freshwater (The EU Water Framework Directive—integrated river basin management for Europe) [15]. Furthermore, the latter method can comprehensively analyze the health of a river using mathematical models, such as the entropy model [16], the cloud model [17], an analytic hierarchy process [18], the matter-element model [19], or the set pair analysis extension model [20]. The TOPSIS (Technique for Order Preference by Similarity to an Ideal Solution) model was proposed by Hwang and Yoon in 1984. It works by calculating the geometric distances of alternatives from the ideal solution. It is used in risk assessments and resource utilization assessments [21,22]. Fuzzy mathematics is used in another comprehensive evaluation method [23]. Among these, the TOPSIS model has been extensively used in river health assessments owing to its numerous advantages, including ease of usage, low information distortion, and freedom from reference sequences. However, this model has certain limitations. In some cases, unreasonable priorities may be obtained, resulting in an inability to effectively distinguish between the pros and cons of the proposal [24]. Considering these limitations, the VIKOR model was proposed, which can effectively express the relative importance of indicators, achieve a balance between overall satisfaction and individual satisfaction, and effectively compensate for the shortcomings of the TOPSIS model [25,26]. However, there have been very few studies investigating the VIKOR method for water evaluations.

The Maotiao River Basin is located in the karst region of the central Guizhou Province, and represents a typical urbanized area in southwest China (Figure 1). Industrial and agricultural areas are well developed in the region, and immigration is high. Under the pressure of intensive urbanization, along with water requirements and competition between users (agriculture, industry, households), the problem of water quality has become multidimensional and critical, especially during scarcity [27]. Therefore, in order to solve the conflicting interests among users, to explore the sources of river pollutants in traditional agricultural areas and enhance agricultural production efficiency, this study combined the fuzzy matter-element model with the VIKOR model. The CRITIC model (criteria importance though intercriteria correlation) and the improved analytical hierarchy process (IAHP) were used to reduce the subjectivity of the water quality assessment process [28]. The aim of this study was to analyze the temporal and spatial characteristics of the water quality of the Maotiao River Basin, based on the fuzzy matter-element–VIKOR model, and a geodetector was used to explore the sources of nutrients in the basin.

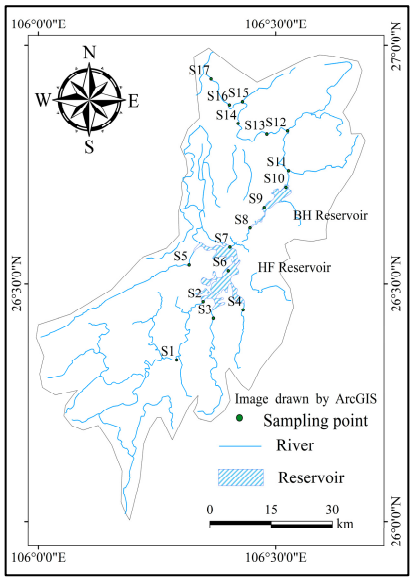

Figure 1. The Maotiao River Basin (Gizhou province, SW China) and sampling sites.

2. Materials and Methods

2.1. Study Area

The Maotiao River, forming the Maotiao River Basin (105°59′–106°22′ E, 26°09′–26°56′ N), is the first-level tributary on the right bank of the middle reaches of the Wujiang River, flowing from south to north through the Pingba District of Anshun City, Qingzhen City of Guiyang City, Guanshan Lake District, Baiyun District, and Xiuwen County, and merging into the Wujiang River in Xiuwen County [29]. The river basin is located in the central part of Guizhou Province, and covers an area of about 3250 km^2. The main stream is 179 km long, and drops for 549 m within the basin, with an average slope of 3%. The climate of the basin is a humid subtropical monsoon climate, with a multi-year averaged temperature of 14.1 °C, an average annual frost-free period of 260–275 days, and multi-year averaged annual precipitation of 1206 mm. The maximum annual precipitation was 1633 mm, and the average reference crop evaporation was between 900 and 1000 mm.

2.2. Sampling and Analysis

In July, August, and November 2020, three sets of samples from 17 locations (S1–S17) were collected (Figure 1). Samples were collected 0.5 m below the water's surface; locations were recorded by a global satellite positioning system (G1388D). Three parallel samples were collected at each sampling location: (a) samples for heavy metal analyses; (b) samples for nutrient analyses; (c) samples for chlorophyll-*a* analyses. Samples for heavy metal analyses were treated with analytical grade nitric acid (HNO_3) immediately after collection to decrease the pH to ≤2: Samples for nutrient and chlorophyll-*a* analyses were not treated with chemicals but immediately placed in a dark cold box (c. 4 °C) for storage and transportation. In the laboratory, samples were stored in a refrigerator at 4 °C. Samples were analyzed within 48 after collection. The samples for heavy metal analyses were filtered through a 0.45 μm membrane filter. Determination of Pb, Ni, and Cu was performed using a flame atomic absorption spectrometer (ZEEnit 7001, Analytical Instruments in Jena, Germany), and a graphite furnace atomic absorption spectrometer (ZEEnit 7001) was used to measure As and Hg. Samples for chlorophyll-*a* were filtered through a cellulose filter. The amount of filtered volume was recorded. Filters were stored in glass vials with acetone for further analyses. Afterwards, the concentrations were determined by colorimetric methods using UV spectrophotometry at 750, 664, 647, and 630 nm. Samples for total nitrogen (TN) and total phosphorus (TP) were collected unfiltered, whereas those for nitrate (NO_3^-), nitrite (NO_2^-), ammonium (NH_3-N), and orthophosphate (PO_4^{3-}) were pre-filtered through membrane filters (0.45 μm). Chemical oxygen demand (COD_{Mn})

was measured by potassium permanganate oxidation method, and the five-day biological oxygen demand (BOD_5) was measured via dilution and inoculation method. All analyses followed standard methods [30]. Prior to each set of analyses, standards with known concentrations of the parameters in question, provided by the National Standards Center, were analyzed to verify accuracy of the instruments and analytical processes. Chemical and biological parameters were analyzed by means of software programs Excel 2019, SPSS 23.0, ArcGIS 10.8, and Origin 2021.

2.3. Statistical Analysis Method

2.3.1. Weight Calculation

The traditional analytic hierarchy process is easily affected by subjective preferences [31]. To avoid this, the judgment matrix was replaced until the consistency check was passed. The transfer matrix was established based on the proportional scale construction method, which eliminates the need to check the consistency of the matrix. The judgment matrix should meet the following conditions: (1) $r_{ij} > 0$; (2) $r_{ij} = 1$; (3) $r_{ij} = 1/r_{ji}$, where r_{ij} is the scale value of the ratio of index i to index j. The scale values used in this study are presented in Table 1.

Table 1. Meaning of scale value.

Scale Value	Meaning
1	Equally important
1.2	Slightly important
1.4	Strongly important
1.6	Obviously important
1.8	Absolutely important

The index factors ($t_1, t_2, \dots$) are sorted in descending order of importance to construct an importance transfer matrix. The two adjacent indicators are compared with each other to determine the degree of importance and marked as t_i; finally, the judgment matrix R is obtained, as shown in Equation (1). With this construction, the matrix always satisfies the consistency test; thus, the subjective weight of the index can be directly calculated without the test, as shown in Equation (2).

$$R = \begin{bmatrix} 1 & t_1 & t_1 t_2 & \cdots & \prod_{i=1}^{n-1} t_i \\ \vdots & & \ddots & & \vdots \\ \frac{1}{\prod_{i=1}^{n-1} t_i} & & \cdots & & 1 \end{bmatrix} \quad (1)$$

$$\alpha_i = \left(\prod_{j=1}^{n} r_{ij} \right)^{\frac{1}{n}} / \sum_{i=1}^{n} \left(\prod_{j=1}^{n} r_{ij} \right)^{\frac{1}{n}} \quad (2)$$

where α_i is the subjective weight of indicator i.

The CRITIC model is an objective weighting method that uses the comparative intensity and conflicts of the indicators to measure their importance. Conflict was measured using the correlation coefficients between pairs of indicators. The comparative intensity was measured by the standard deviation. Equations (3) and (4) were used to normalize indicators, Equation (5) was used to measure the amount of information for the factor, and Equation (6) was used to calculate the objective weight of each indicator.

$$x'_{ij} = \frac{x_{ij}}{max(x_{ij})} \quad (3)$$

$$x'_{ij} = 1 - \frac{x_{ij}}{max(x_{ij})} \tag{4}$$

$$G_i = S_i \sum_j^n (1 - \rho_{ij}) \tag{5}$$

$$\beta_i = \frac{G_i}{\sum_i^n G_i} \tag{6}$$

where ρ_{ij} is the correlation coefficient between indicator i and other indicator, β_i is the objective weight of indicator i, G_i is the information contained in indicator i, and s_i is the standard deviation.

2.3.2. Fuzzy Matter-Element–VIKOR Model

The improved analytic hierarchy process and the CRITIC method were used to determine the weights of the water quality indicators. According to the principle of minimum identification information, a Lagrangian function was established to obtain the combined weights.

The VIKOR method is a complex system based on the multi-criteria decision-making method proposed by Opricovic (1998) [25]. Based on the Hamming and Chebyshev distances, the aggregation function was constructed to show the pros and cons of the proposals. In the matter-element analysis process, for a case M, with respect to the magnitude U of its feature vector C, an ordered triplet R (M, U, C,) is used as the basic unit to describe case M. If the magnitude U is fuzzy, then the triplet is called a fuzzy matter-element.

Equations (7) and (8) were used to calculate grade of membership; then, the composite fuzzy matter-element matrix was established (Equation (9)).

$$u_{(x_{ij})} = \frac{x_{ij}}{max(x_{ij})} \tag{7}$$

when x_{ij} is a positive indicator.

$$u_{(x_{ij})} = \frac{min(x_{ij})}{x_{ij}} \tag{8}$$

when x_{ij} is a negative indicator.

$$R_{MN} = \begin{array}{c|ccc} & M_1 & \cdots & M_m \\ \hline C_1 & u_{11} & \cdots & u_{m1} \\ \vdots & \vdots & \ddots & \vdots \\ C_n & u_{1n} & \ldots & u_{mn} \end{array} \tag{9}$$

The standard fuzzy matter-element R_∇ (Equation (10)) was determined from the maximum and minimum values of the favorable membership degrees of each index in the fuzzy matter-element R_{MN}, and ∇_{ij} represents the square of the difference between the standard fuzzy matter-element matrix and the compound fuzzy matter-element matrix. The difference squared fuzzy matter-element can be described as:

$$R_\nabla = \begin{array}{c|ccc} & M_1 & \cdots & M_m \\ \hline C_1 & \nabla_{11} & \cdots & \nabla_{m1} \\ \vdots & \vdots & \ddots & \vdots \\ C_n & \nabla_{1n} & \ldots & \nabla_{mn} \end{array} \tag{10}$$

To avoid instability of the evaluation results due to changes in the number of solutions, the positive and negative ideal solutions were set as constants:

Positive ideal solution:

$$z^+ = 1 \tag{11}$$

Negative ideal solution:

$$z^- = 0 \tag{12}$$

Weighted Hamming Distance can be expressed as:

$$S_i^+ = \sum_i^n w_i \left(z^+ - x'_{ij} \right). \tag{13}$$

Weighted Chebyshev distance can be expressed as:

$$R_i^+ = max\left(W_i * \left(Z^+ - x'_{ij} \right) \right) \tag{14}$$

where S_i^+ and R_i^+ represent the group effect and individual regret based on the positive ideal solution, respectively.

$$Q_i = v\frac{s_i - mins_i}{maxs_i - mins_i} + (1 - v)\frac{R_i - minR_i}{maxR_i - minR_i} \tag{15}$$

where v is the decision coefficient; $v > 0.5$ indicates that the decision-maker pays more attention to group benefits; $v < 0.5$ indicates that the decision-maker prefers individual regret. However, $v = 0.5$ indicates that the decision-maker has considered group benefits and individual regrets, maintaining a neutral standpoint.

To verify the applicability of the fuzzy matter-element-VIKOR model (FME-VIKOR model) and discuss the stability of the decision result when the decision coefficient V changes, we set the coefficient V to be within an interval of 0.1. For different decision coefficients, the ranking below was analyzed by Spearman correlation and compared with the simple linear weighted (SLW), Technique for Order Preference by Similarity to an Ideal Solution (TOPSIS), and water quality index (WQI).

2.3.3. Geodetector Model

A geodetector is a statistical method used to reveal the spatial differentiation of variables and their driving forces [32]. Compared with traditional factor analysis, geodetectors have evident advantages in analyzing the quantitative contributions of multiple factors, and their interactions. Although geodetectors are mainly used for studying the ecological environment and human health, in recent years, they have been gradually used in studies related to heavy metal pollution, karst rocky desertification, soil organic matter, etc. [33–36]. The geographic detector model is composed of factor detectors, interaction detectors, ecological detectors, and risk detectors. This study mainly uses factor detectors and interaction detectors to reveal the impacts of different types of landscape structure on the water quality of the Maotiao River Basin at different spatial scales.

The factor detector can reveal the degrees of influence of the different types of landscape, i.e., land use and land cover, on the spatial distribution of water quality in the Maotiao River Basin, as the landscape structure had the greatest explanatory power for the spatial differentiation of the water quality index (Equation (15)), when the buffer radius was 1 km. A geodetector can only characterize the degree of factor interpretation and cannot analyze the direction of factor influence. In this study, we used Pearson correlation analysis to determine the direction of influence [37].

3. Results

3.1. Spatiotemporal Characteristics of Water Quality Parameters

3.1.1. Physical Parameters

The temporal and spatial changes in dissolved oxygen (DO), electric conductivity (Cond.), oxidation–reduction potential (ORP), water temperature (WT), and pH during the study period in the Maotiao River Basin are shown in Figure 2. The average concentration of DO in the surface stratum increased from 7.2 mg·L^{-1} (July) to 8.4 mg·L^{-1} (November). The average EC values ranged from 415 to 830 µs·cm^{-1}. In the summer, with a low-water

level, values decreased in the direction of waterflow. The minimum value was 235 μs·cm^{-1} (location S10), and the maximum was 718 μs·cm^{-1} (location S2). In autumn, the EC trend was in the opposite direction. The minimum value was 546 μs·cm^{-1} (location S1), and the maximum value was 830 μS·cm^{-1} (location S14). pH values were relatively stable in July and November, and varied from 7.92 to 8.50 (i.e., slightly alkaline), but values fluctuated considerably in August, when the coefficient of variation was 11.96% and values ranged from acidic (pH5.32 at location S10) to alkaline (pH 8.50 at location S8). In summer, the ORP ranged from −77.8 to −43.5 mv, and the minimum was observed in location S9. However, as the redox conditions of the water in autumn underwent significant changes, the ORP ranged from 157.4 to 234.6 mv, and the water body showed notable oxidation characteristics.

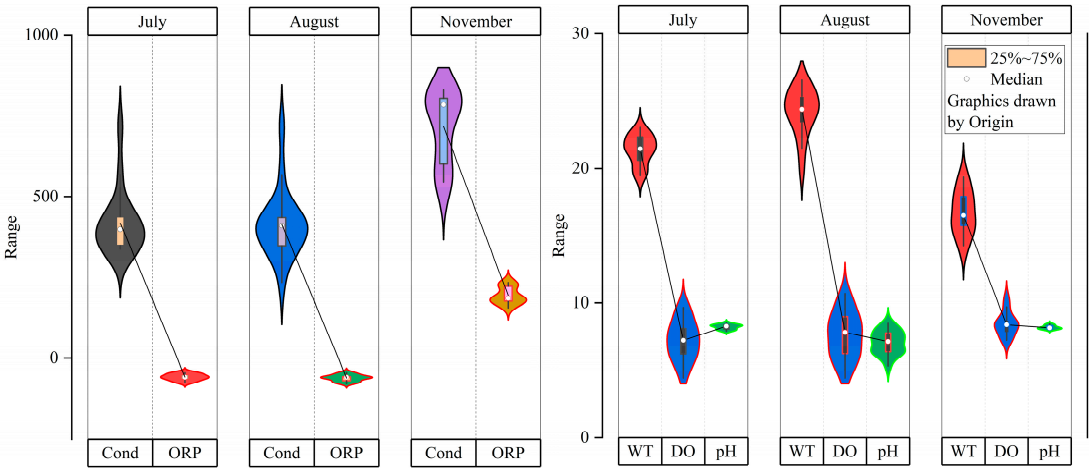

Figure 2. Spatiotemporal values of water quality parameters at 17 locations within the Maotiao River Basin (Gizhou province, SW China) in 2020. Cond: electric conductivity; ORP: oxidation–reduction potential; WT: water temperature; DO: dissolved oxygen; pH: acidity/alkalinity.

WT was consistent with the seasonal changes, and the spatial differences in temperature were small between July and August, but quite large in November, when the wet period started.

3.1.2. Particulate and Dissolved Organic Material

The potassium permanganate index (COD_{Mn}) changed in time and space (Figure 3). During the study period, the average concentration of COD_{Mn} ranged from 1.50 to 1.86 mg·L^{-1}. The maximum value was 3.80 mg·L^{-1} at location S11 in autumn. In general, the concentration of COD_{Mn} had an increasing trend from S1 to S11, but a decreasing trend from S11 to S17.

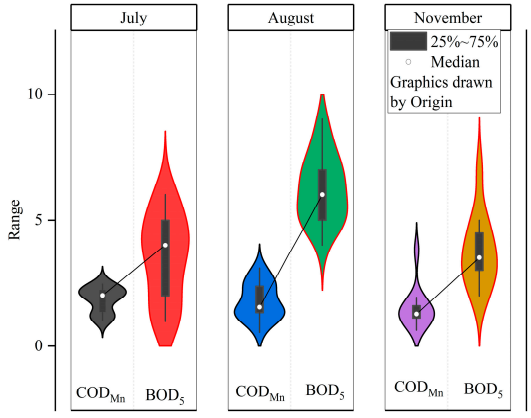

Figure 3. Spatiotemporal values of particulate and dissolved organic material at 17 locations within the Maotiao River Basin (Gizhou province, SW China) in 2020. COD_{Mn}: chemical oxygen demand; BOD_5: five days biological oxygen demand.

3.1.3. Nutrients

Five-day biological oxygen demand (BOD_5) was high: the maximum value in summer was 9.0 mg·L^{-1} (location S3), and in autumn was 7.0 mg·L^{-1} (location S2). In other sampling points, BOD_5 ranged from 3.0 to 5.0 mg·L^{-1}, and exceptionally dropped to 2.0 (locations S12 and S17).

The values of total nitrogen (TN) and total phosphorus (TP) exhibited evident temporal and spatial changes (Figure 4). The TN concentration ranged from 0.95 to 8.47 mg·L^{-1}. The average concentration was 3.05 mg·L^{-1}. The highest and lowest values were observed in autumn at locations S11 and S3, respectively. The nitrate (NO_3^-) concentration ranged from 0.47 to 5.19 mg·L^{-1}. The average concentration was 2.19 mg·L^{-1}. The nitrite (NO_2^-) concentration ranged from below the level of detection (LoD) to 0.61 mg·L^{-1}. The average concentration was 0.08 mg·L^{-1}. The ammonium (NH_4^+-N) concentration ranged from 0.01 to 2.92 mg·L^{-1}. The average concentration was 0.34 mg·L^{-1}. NO_3^- represented, during the study period, between 45% and 90% of the total nitrogen present in the water bodies, whereas the proportions of inorganic nitrogen from the remaining two forms were low (Figure 4).

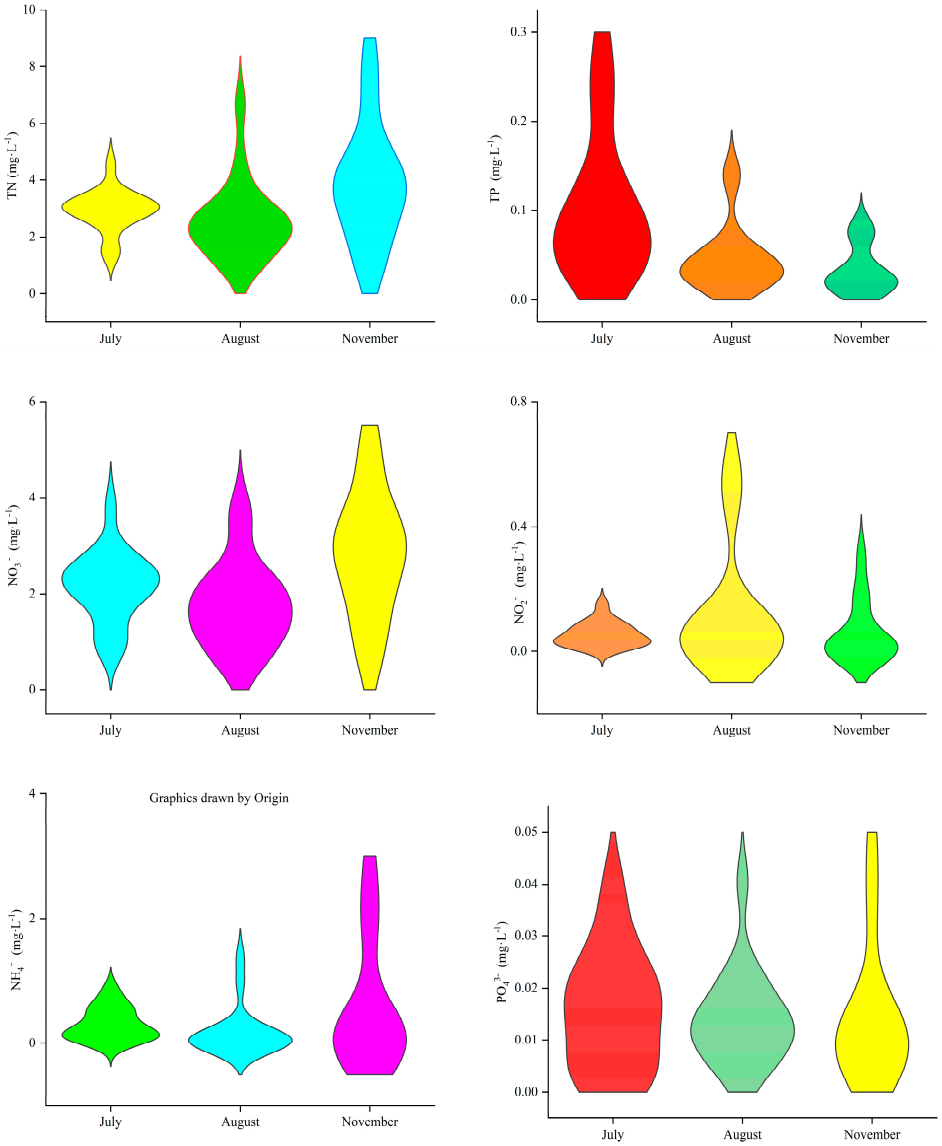

Figure 4. Nutrients concentrations at 17 locations within the Maotiao River Basin (Gizhou province, SW China) in 2020. TN: total nitrogen; NO_3^-: nitrate; NO_2^-: nitrite; NH_4^+: ammonium; TP: total phosphorus; PO_4^{3-}: orthophosphate.

The average TP concentration was 0.01 to 0.30 mg·L^{-1}. The average concentration was 0.06 mg·L^{-1}. The highest concentration appeared in July, and the lowest in November. The orthophosphate (PO_4^{3-}) concentration ranged from LoD to 0.05 mg·L^{-1}. The average concentration was 0.01 mg·L^{-1}. The highest concentration was found in November, whereas the lowest values appeared in summer. Moreover, the upstream TP concentration was significantly lower than in the downstream locations. The PO_4^{3-} concentration in the river was significantly higher than in the reservoirs, indicating that the phytoplankton in the reservoirs more efficiently utilized orthophosphate than phytobenthos in the rivers.

The chlorophyll-*a* concentration indicated a seasonal trend (Figure 5). It increased in summer and decreased in autumn, and the increase of primary producers (i.e., unicellular algae and their colonies and macrophytes) in the reservoirs was considerably higher than in the rivers. The maximum concentration of chlorophyll-*a* (Chl-*a*) was found in summer at location S7 (36.7 mg·m^{-3}), whereas the minimum was at location S14 (1.4 mg·m^{-3}) in November.

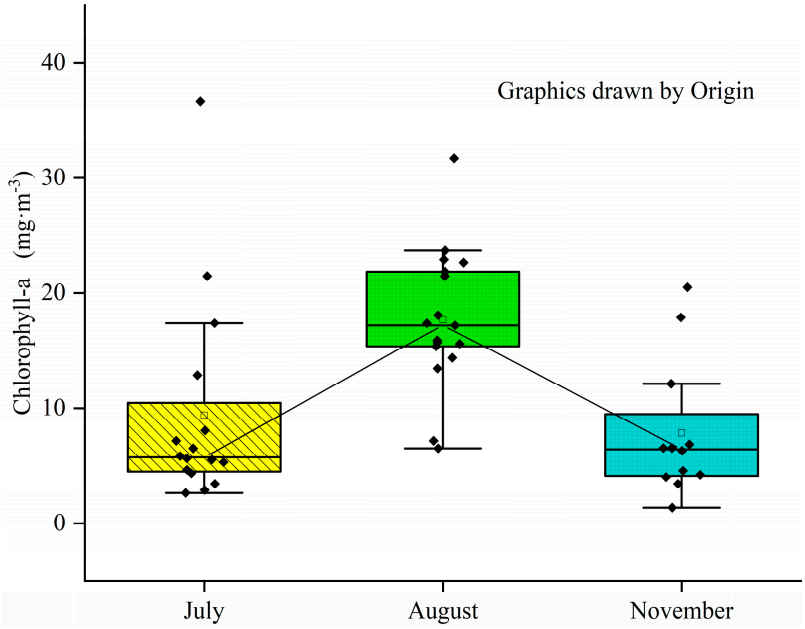

Figure 5. Spatiotemporal values of chlorophyll-*a* concentration at 17 locations within the Maotiao River Basin (Gizhou province, SW China) in 2020.

3.1.4. Heavy Metals

Arsenic (As), chromium (Cr), copper (Cu), mercury (Hg), nickel (Ni), and lead (Pb) had evident temporal and spatial distribution dynamics (Figure 6). The concentration of Hg varied from below the LoD to 0.03 μg·L^{-1}. The average concentration was 0.01 μg·L^{-1}. The lowest concentration was found in August (location S17) and the highest in July (location S4). The As concentration varied from 0.22 to 2.38 μg·L^{-1}. The average concentration was 1.12 μg·L^{-1}. The minimum concentration was found in July (location S2), and the maximum concentration was found in August (location S17). The Cr concentration varied from LoD to 9.78 μg·L^{-1}. The average concentration was 5.07 μg·L^{-1}. The Cu concentration varied from 0.80 to 4.87 μg·L^{-1}. The average concentration was 2.81 μg·L^{-1}. The maximum and minimum values were in July at locations S9 and S6, respectively. The Ni concentration varied from 3.46 to15.36 μg·L^{-1}. The average concentration was 5.84 μg·L^{-1}. The maximum and minimum values were in August at locations S10 and S17, respectively. The Pb concentration varied from 0.07 to 0.24 μg·L^{-1}. The average concentration was 0.16 μg·L^{-1}. The maximum and minimum values were found in July at locations S8 and S2, respectively.

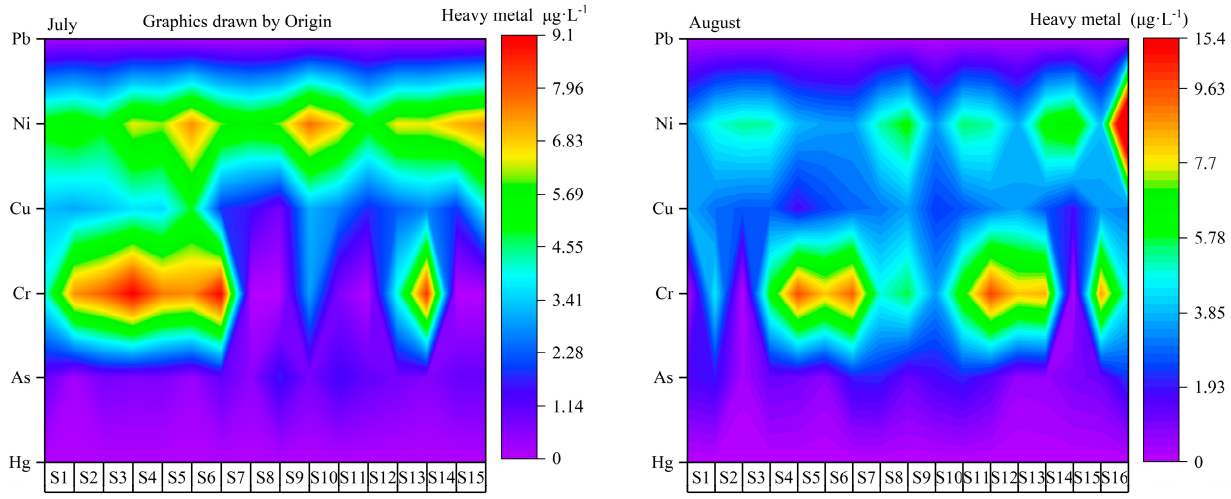

Figure 6. Spatiotemporal distribution of heavy metal concentration at 17 locations within the Maotiao River Basin (Gizhou province, SW China) in 2020.

Two heavy metals, Cr and Ni, were the dominating pollutants in the Maotiao River Basin (Figure 6). Along the river's course, the dissolved Ni concentration significantly decreased. The values of Cr concentrations were shifted downstream, where its concentrations significantly increased between locations S12 and S13.

3.2. Spatial Distribution of Land Use Structures

Among the types of landscape in the Maotiao River Basin, the agricultural area was the largest, and accounted for 49.74% of the total watershed area, followed by forest (26.31%), grassland (9.68%), and urban (7.01%) areas (Figure 7). Shrublands and water bodies were the smallest, accounting for 5.38% and 1.69%, respectively. As the buffer zone area increased, as strips of land around the water bodies, from 100 m (a standard distance) to 5 km (this study), the proportion of agricultural areas in the buffer zone increased from 22.8% to 44.8%, and that of forest increased from 15.03% to 33.00%. The proportions of shrubland and urban areas reached their maxima when the buffer zone was set at 900 m, which were 6.30% and 3.10%, respectively. The proportions of grassland and water continued to decrease, indicating that as the river buffer zone increasesd, the types of land use also changed significantly, and the landscape pattern underwent significant changes. Meanwhile, urban areas along the Maotiao River are primarily concentrated near locations S8 and S9, respectively, and are relatively far from the river. From the perspective of spatial changes in land use structures, with the expansion of the buffer zone, human activity in the Maotiao River Basin has gradually increased.

3.3. Comprehensive Evaluation of Water Quality Based on the Fuzzy Matter-Element-VIKOR Model

The improved analytical hierarchy process (IAHP) has strong subjectivity and is affected by the knowledge of the decision-making participants. The subjective weights of chlorophyll-*a* and TP for the basin in 2020 were set at 0.44 and 0.24, respectively (Figure 8), indicating that the current water environmental management of the basin is focused on controlling phosphorus emissions and preventing water eutrophication. On the basis of the CRITIC model, the objective weights of Chl-*a*, TP, TN, COD_{Mn}, EC, and DO were 0.20, 0.18, 0.16, 0.16, 0.16, and 0.14, respectively. Among them, Chl-*a* and TP had the greatest impacts on the decision-making results, but compared with the IAHP method, the levels of importance of the water quality indicators were relatively close. The weights of Chl-*a* and TP significantly reduced; the weights of EC, DO, and COD_{Mn} increased significantly; and the weights of TN increased slightly. By combining the advantages of subjective and objective weights, the results showed that the primary productivity of aquatic plants,

as a result of N and P concentrations, is of great significance to environmental water management.

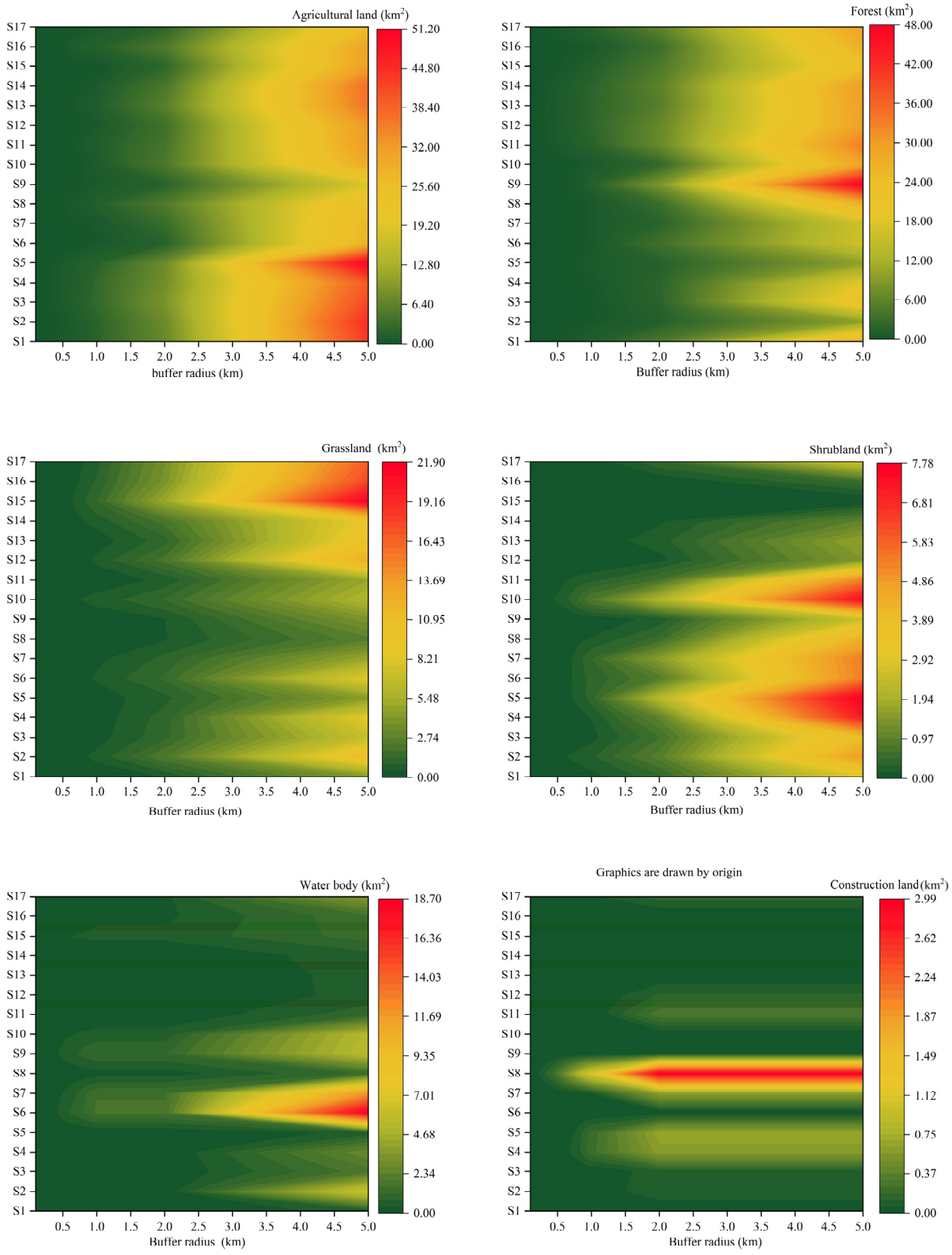

Figure 7. Land use structure at 17 locations within the Maotiao River Basin (Gizhou province, SW China) in 2020.

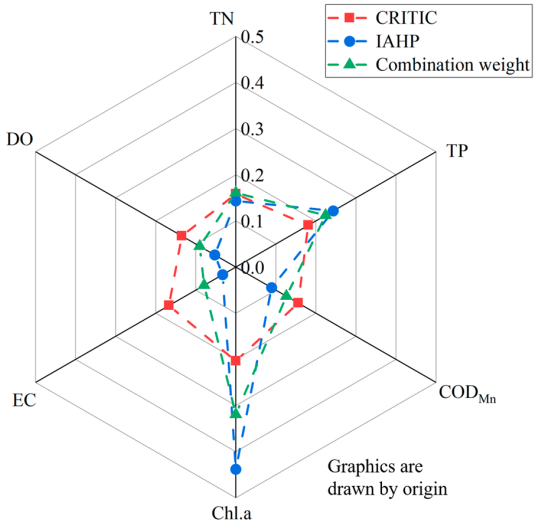

Figure 8. The weight composition of the water quality index of the Maotiao River Basin (Gizhou province, SW China) in 2020, based on three different models: CRITIC, IAHP, and combined. TN: total nitrogen; TP: total phosphorus; COD_{Mn}: chemical oxygen demand; Chl.a: chlorophyll-*a*; EC: electric conductivity; DO: dissolved oxygen. According to the fuzzy matter-element–VIKOR model, TN, DO, TP, EC, COD_{Mn}, and Chl-*a* were selected to calculate the aggregation function Q (Equation (15)). The water quality of the Maotiao River Basin in July was generally low (Figure 9). The low-value areas were mainly distributed in the HF Reservoir (locations S6, S7) and the Yangchang River (location S2) in spots, and their water quality index values were lower than 0.08; high value areas mainly included areas near locations S8, S14, and S16, where the water quality index values were 0.67, 0.50, and 0.60 respectively. The water quality of the Maotiao River Basin further decreased in August, and the low-quality areas were distributed in blocks, mainly concentrated in the lower reaches of the Maotiao River, including locations S8 (0.16), S9 (0.19), S10 (0.21), S11 (0.004), S12 (0.14), S13 (0.18), and S16 (0.20), whereas the high-value areas were mainly distributed in the HF Reservoir [38]. The water quality of the river was significantly improved in November, and the low-value areas shrank from south to north; they were distributed in points, mainly in locations S11 (0.28), S12 (0.31), and S13 (0.02). The high-value areas significantly expanded from north to south, including locations S1 (0.50), S2 (0.65), and S3 (0.45), and were spatially high in the south and low in the north.

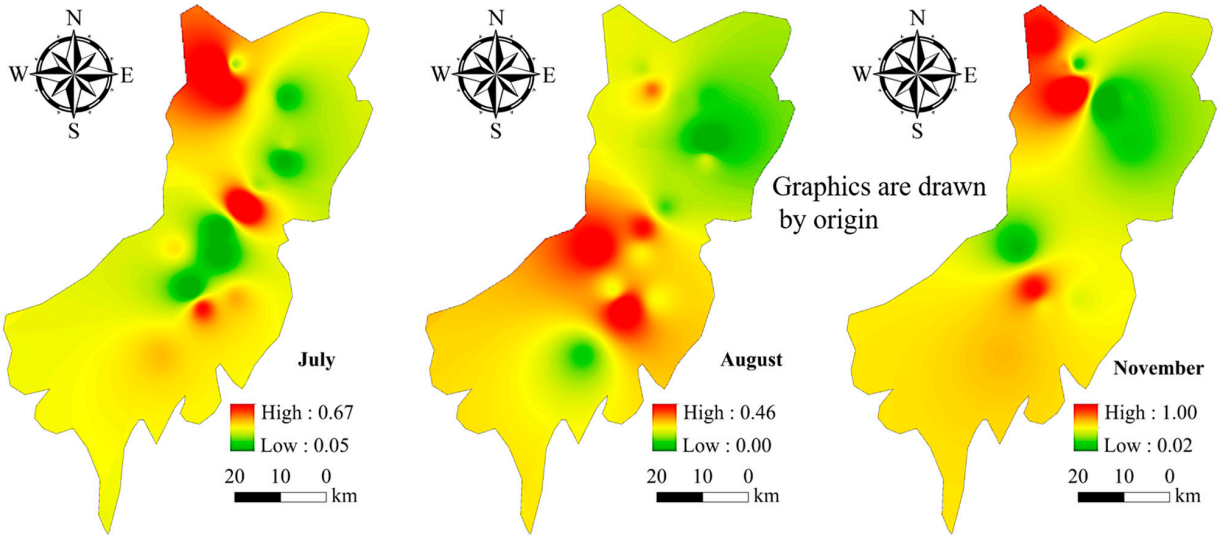

Figure 9. Spatiotemporal characteristics of water quality in the Maotiao River Basin (Gizhou province, SW China) in 2020 based on the VIKOR model.

3.4. Relationships between Land Cover and Water Quality

3.4.1. Factor Detector

The analysis of factor detector revealed that the factors affecting the spatiotemporal changes in the water quality of the basin during different periods have relatively significant effects (Table 2). In July, August, and November, agricultural land use, which was the main factor affecting water quality changes, had effect intensity values of 0.72, 0.60, and 0.80, respectively. The effect intensity of urban land use decreased from 0.381 to 0.054. The effect of water areas was the strongest in July (0.69) and the weakest in August (0.09). The maximum factor intensities of forested areas and shrublands were 0.34 and 0.50, respectively, both observed in August. However, the change in the effect intensity of grassland showed an opposite trend, with the minimum value being 0.10 in August.

Table 2. Factor analysis results by type of landscape and water quality characteristics in the Maotiao River Basin (Gizhou province, SW China) in 2020.

	Agriculture	Forest	Grassland	Shrub Land	Water Bodies	Impervious Surfaces
July	0.724	−0.062	−0.491	−0.493	−0.693	0.381
August	0.600	−0.325	0.104	0.498	0.086	−0.242
November	0.798	−0.137	0.452	−0.076	−0.119	−0.054

3.4.2. Interaction Detector

The interactions among agricultural areas and forests, shrubs, and water bodies exceeded 0.90 in July, showing bivariate or nonlinear enhancement (Figure 10). The interactions were far greater than the impact of a single factor. In August, the interaction intensities of shrubland and cultivated land, and arable land and woodland, were 0.98 and 0.91, showing bivariate enhancement and nonlinear enhancement, respectively. The interaction intensities in autumn of arable land and forest; grassland and cultivated land; and water body and cultivated land were 0.999, 0.96, and 0.94, respectively, all showing bivariate enhancement.

3.5. Sensitivity Analysis

With an increase in the decision-making coefficient V (Equation (15)), the correlations between the decision-making results at different standpoints gradually decreased, indicating that the subjective positions of people in multi-dimensional decision-making have a great impact on the decision-making results (Figure 11). However, the results of the Spearman correlation analysis indicated that although the coefficient V was constantly changing, there was a highly significant correlation between the different ranking results of the FME–VIKOR model [39]. This study maintains neutrality in multi-dimensional decision-making based on the principle of attribute compromise; that is, when $V = 0.5$, the ranking result of the FME–VIKOR model was used as the basis for decision-making [40]. The correlation between the FME–VIKOR model and other ranking results was greater than 0.95 ($p < 0.01$), indicating that the model was stable for water quality discrimination, and the ranking results were essentially the same as the results of the SLW, TOPSIS, and WQI models. We found that as the decision coefficient V increased in the FME–VIKOR model, the coefficient of variation of the aggregation function Q decreased from 81.85% to 54.43%, whereas the coefficients of variation of the SLW, TOPSIS, and WQI models were 13.26%, 17.94%, and 12.6%, respectively—much lower than those of the FME–VIKOR model. Among them, WQI had the lowest degree of discrimination for water quality evaluation results, primarily because the essence of its modeling idea is based on the Delphi method. The water quality parameters were divided into intervals, and the parameters of different intervals were directly assigned. Thus, the proposed method was used to perform a preliminary assessment of the water quality. The smaller the number of hierarchical gradients of water quality parameters, the greater the ambiguity of the result.

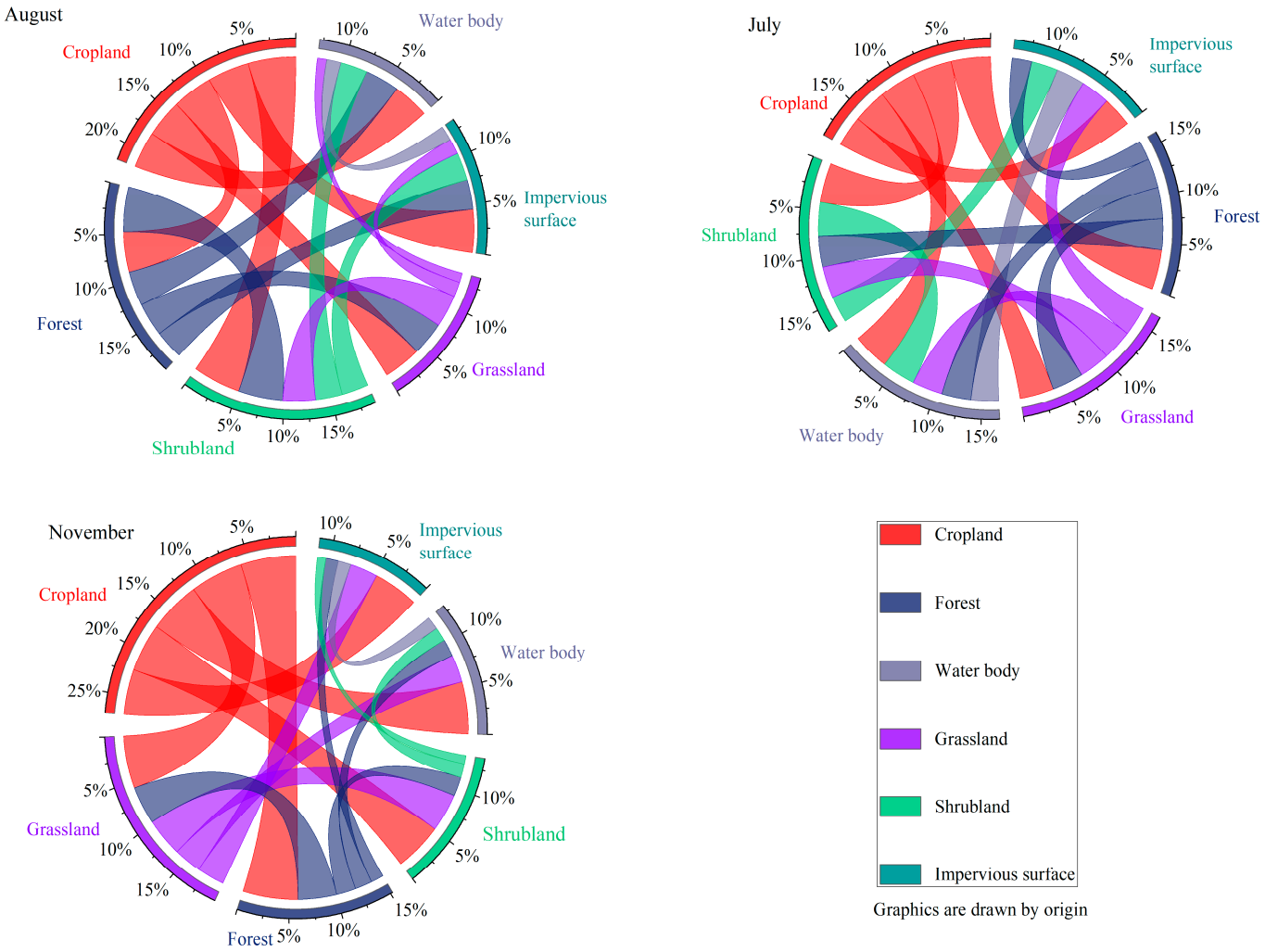

Figure 10. Interactive factor analysis results by type of landscape and water quality characteristics in the Maotiao River Basin (Gizhou province, SW China) in 2020.

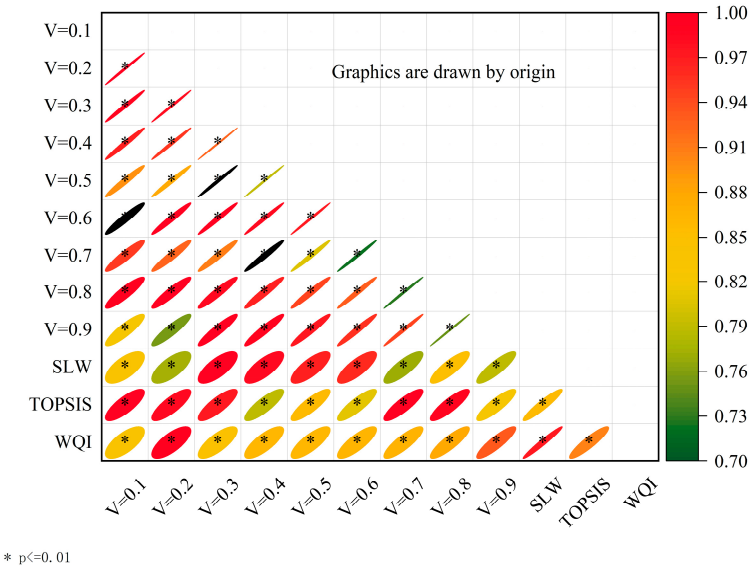

Figure 11. Sensitivity analysis of evaluation in the Maotiao River Basin (Gizhou province, SW China) in 2020.

4. Discussion

In a changing environment, water quality is a complex process controlled by a variety of factors. The use of interaction detectors to reveal the degrees of influence of variables provides a powerful tool for the application of effective measurements for control of water quality pollutants. The most intuitive representation of changes in the terrestrial environment, as a result of human activities, is analysis of the types of land cover and land use. According to the results of the present geographical detector analysis, urban areas had a negative correlation with water quality in the dry season, because wastewater is less diluted by runoff, and rivers and lakes have become important recipients of pollutants. This results in negative effects correlated with higher temperature and low precipitation [41–43]. However, in this study, the impact of urban areas on water quality was weak, with a factor influence of <0.39. The urban areas in the Maotiao River Basin are mainly distributed in the areas surrounding the Hongfeng and the Baihua reservoirs, which are mainly affected by point source pollution. Upstream river sections are affected by agriculture. Heavy metal pollution in suspended material is heavily dependent on precipitation and waterflow, although their distribution is dependent on species (Figure 6). Along the river, the concentrations of some species increased, and those of some species decreased. Local concentrations could be attributed to the subtropical monsoon climate that has evident impacts on transport of fine suspended material associated with heavy metals through erosion and deposition. In July, Guizhou Province experiences a rainy season, during which surface runoff carries cations to rivers attached to fine suspended inorganic and/or organic particles and increases the concentrations of heavy metals there. When the rainfall belt shifted northward, the area was gradually controlled by the subtropical high-pressure zone, and the dilution effect of the runoff on the pollutants gradually weakened, resulting in pollution diffusion. Water body evapotranspiration activities were vigorous, and the concentrations of dissolved heavy metals also decreased accordingly due to reduced runoff into the rivers or sedimentation processes within the reservoirs. The reservoirs become important deposition regions for this type of pollutants during the dry season, which deteriorates the water quality of the lakes [44]. The spatial club effect of dissolved Cr was evident from its distribution in August. Except for S17, high-value areas were distributed in reservoirs, and the level of Cr in the rivers entering the reservoir was significantly reduced, indicating that the source of it was heavily dependent on leaching from terrestrial areas.

In order to increase yield, chemical fertilizers and pesticides are widely used in agriculture, which increase the concentrations of N, P, and heavy metals in water bodies and cause the deterioration of water quality. As example of an indicator of water quality is BOD_5, which is among the standard parameters correlated with eutrophication (presence of T and P compounds). According to China's surface water environmental quality standard (GB3838-2002), in July, the BOD_5 values were <3.0 $mg \cdot L^{-1}$—water quality Class II—in 12 (out of 17) locations; and five locations, where values ranged from 4.0 to 6.0 $mg \cdot L^{-1}$, belonged to water quality Class IV. In August, watery quality decreased, as seven locations (S1, S3, S4, S9, S10, S13, S14) moved to water quality Class V, representing 41.18% of the total number of sampling points.

However, it should be noted that although the agricultural land use in the basin plays a leading role in the spatial distribution of water quality along the rivers, there was some positive succession. This contradiction may be related to changes in the ecological efficiency of agricultural production [45]. Agricultural land use has a multi-dimensional impact on river pollution. Agricultural production has improved in Guizhou Province, based on the strategy of comprehensively managing different types of land use, and both terrestrial and aquatic habitats. Ecological agricultural production has been gradually moved toward a new model, which reduces the concentrations of pollutants at their sources. The diversification of crops and maintaining natural vegetation also contribute to the potential of biological retention and the transformation of pollutants.

Arable land in the basin is mainly distributed in the upper reaches of the river, where the terrain is flat and the runoff velocity is slow, which indirectly prolongs the discharge time, increasing the potential for adsorption of water pollutants on soil particles, and it provides temporary opportunities to reduce the concentration of pollutants in the river. During monsoon precipitation, some erosion occurred in the terrestrial zone, forming fine sediment on the river bed, which was transported downstream, where after entering reservoirs, much of it sunk into the sediment.

Fang et al. reported that as the slope increases, the loss of N and P in the soil is greater. Actively adopting soil conservation measures is important in order to hinder runoff erosion and slow down waterflow [46]. Wu and Lu also reported that relief affects land use through insolation, heat, water resources, soil retention capability, and soil structure, thereby affecting the spatial distributions of pollution sources. The composition of the landform mainly affects the speed, direction of flow, and diffusion of pollutants [42,47–49]. In this study, the forested areas and the spatial distribution of water quality had a negative relation, which is different from what previous studies have found. This study showed that forested areas have an important interception effect on N, P, and other pollutants. However, within the 1 km buffer zone within the basin, as the fragmentation of the landscape is relatively large, the adsorption and interception of pollutants by natural vegetation was weakened [50–52]. At the same time, accumulations of litter and fallen leaves may cause the buildup of refractory organic matter during the biological decomposition process and flow into the river along with runoff. This observation was consistent with that from the study by Zhou et al. [53]. In the Maotiao River Basin, the region is dominated by karst landforms with thin soil layers and short vegetation, which are not conducive to the growth of forests. Forest is mainly present in areas with steep terrain, and surface runoff was an important contributor to the loss of soil TN and TP.

5. Conclusions

The results obtained by the fuzzy matter-element–VIKOR model showed that the pollutant concentrations in Maotiao River Basin were affected by precipitation and were low in the wet period and high in the dry period. Geographical detector analysis revealed that agricultural land use was the main factor influencing the spatial changes in the water quality of the river. The comparison of area size between agricultural land and forest could explain 99% of the spatial differentiation of water quality, whereas the contribution of urban areas was low. Based on the findings of this study, we conclude that good and coordinated agricultural management techniques and the construction of interception dams, fish-scale pits, and other water and soil conservation projects within the river basin would be a great move forward to improve river water quality. However, this study still has some limitations. For example, river water quality is a constantly changing thing, and long-term series studies may be more effective at explaining the sources of pollutants in water bodies.

Author Contributions: Conceptualization, Y.L.; Writing-Original Draft, Y.L. and Q.L.; Methodology, Y.L.; Writing-Review, C.L., L.Y., G.H. and A.B.; Supervision, Q.L. and S.J.; Software, Q.L. and S.J.; Investigation, Y.L., S.Z. and M.H. Data Curation, Q.L., S.J., S.Z. All authors have read and agreed to the published version of the manuscript.

Funding: This work was financed by the Special Foundation for National Science and the Technology Basic Research Program of China grant number [2019FY101900], and the Science and Technology Foundation of Guizhou Province grant number ([2020]6009, [2020]4Y009, [2020]080, [2020]1Y252), and funded by the Slovenian Research Agency grant number [ARRS program P1-0255].

Data Availability Statement: The data for this study are available through the corresponding author.

Conflicts of Interest: The authors declare that they have no known competing financial interest or personal relationships that could have appeared to influence the work reported in this paper.

References

1. Soriano, C. On the Anthropocene formalization and the proposal by the Anthropocene Working Group. *Geol. Acta* **2020**, *18*, 1–10. [CrossRef]
2. Zając, Z.; Sędzikowska, A.; Maślanko, W.; Woźniak, A.; Kulisz, J. Occurrence and Abundance of *Dermacentor reticulatus* in the Habitats of the Ecological Corridor of the Wieprz River, Eastern Poland. *Insects* **2021**, *12*, 96. [CrossRef]
3. Yang, C.Y.; Zhou, Y.; Chen, Y.; Wang, L.W. Practice exploration of ecological protection and restoration of mountains, rivers, forests, fields, lakes and grasses based on NbS. *Earth Sci. Front.* **2021**, *28*, 25–34.
4. Bi, Y.j.; Zhao, J.; Zhang, W.G.; Zhao, Y. Simulation of hydrological cycle for mountain-water-forest-cropland-lake-grass system in Hetao region, Inner Mongolia of China by WACM4.0 model. *Trans. Chin. Soc. Agric. Eng. (Trans. CSAE)* **2020**, *36*, 148–158. [CrossRef]
5. Ouyang, J.; Zhang, K.Z.; Wen, B.; Lu, Y. Top-Down and Bottom-Up Approaches to Environmental Governance in China: Evidence from the River Chief System (RCS). *Int. J. Environ. Res. Public Health* **2020**, *17*, 7058. [CrossRef]
6. Zhou, L.; Li, L.-Z.; Huang, J.-K. The river chief system and agricultural non-point source water pollution control in China. *J. Integr. Agric.* **2021**, *20*, 1382–1395. [CrossRef]
7. Wu, C.; Ju, M.; Wang, L.; Gu, X.; Jiang, C. Public Participation of the River Chief System in China: Current Trends, Problems, and Perspectives. *Water* **2020**, *12*, 3496. [CrossRef]
8. Shen, K.R.; Jin, G. The Policy Effects of the Environmental Governance of Chinese Local Governments: A Study Based on the Progress of the River Chief System. *Soc. Sci. China* **2020**, *41*, 87–105.
9. Tang, Y.; Zhao, X.; Jiao, J. Ecological security assessment of Chaohu Lake Basin of China in the context of River Chief System reform. *Environ. Sci. Pollut. Res.* **2020**, *27*, 2773–2785. [CrossRef]
10. Liu, H.; Chen, Y.D.; Liu, T.; Lin, L. The River Chief System and River Pollution Control in China: A Case Study of Foshan. *Water* **2019**, *11*, 1606. [CrossRef]
11. Petesse, M.L.; Siqueira-Souza, F.K.; Freitas, C.E.D.C.; Petrere, M. Selection of reference lakes and adaptation of a fish multimetric index of biotic integrity to six amazon floodplain lakes. *Ecol. Eng.* **2016**, *97*, 535–544. [CrossRef]
12. Hering, D.; Feld, C.K.; Moog, O.; Ofenböck, T. Cook book for the development of a Multimetric Index for biological condition of aquatic ecosystems: Experiences from the European AQEM and STAR projects and related initiatives. In *The Ecological Status of European Rivers: Evaluation and Intercalibration of Assessment Methods*; Springer: Dordrecht, The Netherlands, 2006.
13. Zhang, X.; Meng, Y.; Xia, J.; Wu, B.; She, D. A combined model for river health evaluation based upon the physical, chemical, and biological elements. *Ecol. Indic.* **2018**, *84*, 416–424. [CrossRef]
14. Lin, L.; Wang, F.; Chen, H.; Fang, H.; Zhang, T.; Cao, W. Ecological health assessments of rivers with multiple dams based on the biological integrity of phytoplankton: A case study of North Creek of Jiulong River. *Ecol. Indic.* **2021**, *121*. [CrossRef]
15. WFD. The EU Water Framework Directive—Integrated River Basin Management for Europe. European Commission. 2020. Available online: http://ec.europa.eu/environment/water/water-framework/index_en.html (accessed on 23 October 2000).
16. Deng, X.; Xu, Y.; Han, L.; Yu, Z.; Yang, M.; Pan, G. Assessment of river health based on an improved entropy-based fuzzy matter-element model in the Taihu Plain, China. *Ecol. Indic.* **2015**, *57*, 85–95. [CrossRef]
17. Yang, Z.; Wang, Y. The cloud model based stochastic multi-criteria decision making technology for river health assessment under multiple uncertainties. *J. Hydrol.* **2020**, *581*, 124437. [CrossRef]
18. Qin, Z.; Li, H.; Liu, Z. Multi-objective comprehensive evaluation approach to a river health system based on fuzzy entropy. *Math. Struct. Comput. Sci.* **2014**, *24*, E240515. [CrossRef]
19. Xue, C.; Shao, C.; Chen, S. SDGs-Based River Health Assessment for Small- and Medium-Sized Watersheds. *Sustainability* **2020**, *12*, 1846. [CrossRef]
20. Wan, X.; Yang, T.; Zhang, Q.; Yan, X.; Hu, C.; Sun, L.; Zheng, Y. A novel comprehensive model of set pair analysis with extenics for river health evaluation and prediction of semi-arid basin—A case study of Wei River Basin, China. *Sci. Total. Environ.* **2021**, *775*, 145845. [CrossRef] [PubMed]
21. Guo, W.; Wang, H. Application of TOPSIS Model Based on AHP Weight to Beiyun River Ecosystem Health Assessment. *Energy Procedia* **2011**, *11*, 3899–3904. [CrossRef]
22. Seyedmohammadi, J.; Sarmadian, F.; Jafarzadeh, A.A.; Ghorbani, M.A.; Shahbazi, F. Application of SAW, TOPSIS and fuzzy TOPSIS models in cultivation priority planning for maize, rapeseed and soybean crops. *Geoderma* **2018**, *310*, 178–190. [CrossRef]
23. Zhao, Y.W.; Zhou, L.Q.; Dong, B.Q.; Dai, C. Health assessment for urban rivers based on the pressure, state and response framework—A case study of the Shiwuli River. *Ecol. Indic.* **2019**, *99*, 324–331. [CrossRef]
24. Zeng, S.; Chen, S.-M.; Fan, K.-Y. Interval-valued intuitionistic fuzzy multiple attribute decision making based on nonlinear programming methodology and TOPSIS method. *Inf. Sci.* **2020**, *506*, 424–442. [CrossRef]
25. Duckstein, L.; Opricovic, S. Multiobjective optimization in river basin development. *Water Resour. Res.* **1980**, *16*, 14–20. [CrossRef]
26. Opricovic, S.; Tzeng, G.-H. Compromise solution by MCDM methods: A comparative analysis of VIKOR and TOPSIS. *Eur. J. Oper. Res.* **2004**, *156*, 445–455. [CrossRef]
27. Liu, D.; Zhang, G.; Li, H.; Fu, Q.; Li, M.; Faiz, M.A.; Ali, S.; Li, T.; Khan, M.I. Projection pursuit evaluation model of a regional surface water environment based on an Ameliorative Moth-Flame Optimization algorithm. *Ecol. Indic.* **2019**, *107*, 105674. [CrossRef]

28. Zhang, Q.; Xu, P.; Qian, H. Groundwater Quality Assessment Using Improved Water Quality Index (WQI) and Human Health Risk (HHR) Evaluation in a Semi-arid Region of Northwest China. *Expo. Health* **2020**, *12*, 487–500. [CrossRef]
29. Xu, Y.; Luo, D.; Peng, J. Land use change and soil erosion in the Maotiao River watershed of Guizhou Province. *J. Geogr. Sci.* **2011**, *21*, 1138–1152. [CrossRef]
30. American Public Health Association. *Standard Methods for the Examination of Water and Wastewater*, 19th ed.; American Public Health Association: Washington, DC, USA, 1998.
31. Abrahamsen, E.B.; Milazzo, M.F.; Selvik, J.T.; Asche, F.; Abrahamsen, H.B. Prioritising investments in safety measures in the chemical industry by using the Analytic Hierarchy Process. *Reliab. Eng. Syst. Saf.* **2020**, *198*, 106811. [CrossRef]
32. Wang, J.F.; Zhang, T.L.; Fu, B.J. A measure of spatial stratified heterogeneity. *Ecol. Indic.* **2016**, *67*, 250–256. [CrossRef]
33. Gu, H.; Fan, W.; Liu, K.; Qingwu, J.; Li, X.; Jiang, J.; Chen, E.; Zhou, Y.; Jiang, Q. Spatio-temporal variations of typhoid and paratyphoid fevers in Zhejiang Province, China from 2005. *Sci. Rep.* **2017**, *7*, 1–11. [CrossRef]
34. Zhang, J.; Mu, G.; Zhang, Z.; Huang, X.; Fang, H. Speciation Variation and Bio-Activation of Soil Heavy Metals (Cd and Cr) in Rice-Rape Rotation Lands in Karst Regions. *Int. J. Environ. Res. Public Health* **2021**, *18*, 1364. [CrossRef] [PubMed]
35. Luo, X.L.; Wang, S.J.; Bai, X.Y.; Tan, Q.; Ran, C.; Chen, H.; Xi, H.P.; Chen, F.; Cao, Y.; Wu, L.H.; et al. Analysis on the spatio-temporal evolution process of rocky desertification in Southwest Karst area. *Acta Ecol. Sin.* **2021**, *41*, 680–693.
36. Du, Z.; Gao, B.; Ou, C.; Du, Z.; Yang, J.; Batsaikhan, B.; Dorjgotov, B.; Yun, W.; Zhu, D. A Quantitative Analysis of Factors Influencing Organic Matter Concentration in the Topsoil of Black Soil in Northeast China Based on Spatial Heterogeneous Patterns. *ISPRS Int. J. Geo-Inf.* **2021**, *10*, 348. [CrossRef]
37. Huang, X.-G.; Zhao, J.-B.; Cao, J.-J.; Song, Y.-Y. Spatial-temporal Variation of Ozone Concentration and Its Driving Factors in China. *Huan Jing Ke Xue Huanjing Kexue* **2019**, *40*, 1120–1131.
38. Li, Q.H.; Han, L.B.; Ma, Y.M.; Liu, Y.L. The relationship between and cyanobacterial composition characteristics environmental factors in Hongfeng Reservoir of Guizhou Plateau. *J. Guizhou Norm. Univ. (Nat. Sci. Ed.)* **2021**, *39*, 1–7. [CrossRef]
39. Akram, M.; Kahraman, C.; Zahid, K. Group decision-making based on complex spherical fuzzy VIKOR approach. *Knowl.-Based Syst.* **2021**, *216*, 106793. [CrossRef]
40. Zhang, H.; Lu, M.; Ke, X.; Yu, S.; Zhao, J.; Wu, Y.; Cheng, L.; Li, X. Evaluation model of black-start schemes based on optimal combination weights and im-proved VIKOR method. *Int. J. Electr. Power Energy Syst.* **2021**, *129*, 106762. [CrossRef]
41. Zhao, J.; Lin, L.; Yang, K.; Liu, Q.; Qian, G. Influences of land use on water quality in a reticular river network area: A case study in Shanghai, China. *Landsc. Urban Plan.* **2015**, *137*, 20–29. [CrossRef]
42. Shehab, Z.N.; Jamil, N.R.; Aris, A.Z.; Shafie, N.S. Spatial variation impact of landscape patterns and land use on water quality across an urbanized watershed in Bentong, Malaysia. *Ecol. Indic.* **2021**, *122*, 107254. [CrossRef]
43. Huang, W.; Mao, J.; Zhu, D.; Lin, C. Impacts of Land Use and Land Cover on Water Quality at Multiple Buffer-Zone Scales in a Lakeside City. *Water* **2019**, *12*, 47. [CrossRef]
44. Huang, B.S.; Li, S.L.; Qiu, J.; Hu, P.; Liu, D. The theory of dirty basin—A new method of surface water resources evaluation considering influence of river and lake water quality. *J. Hydraul. Eng.* **2021**, *52*, 150–157.
45. Yu, S.; Xu, Z.; Wu, W.; Zuo, D. Effect of land use types on stream water quality under seasonal variation and topographic characteristics in the Wei River basin, China. *Ecol. Indic.* **2016**, *60*, 202–212. [CrossRef]
46. Fang, H. Effect of soil conservation measures and slope on runoff, soil, TN, and TP losses from cultivated lands in northern China. *Ecol. Indic.* **2021**, *126*, 107677. [CrossRef]
47. Wu, J.; Lu, J. Spatial scale effects of landscape metrics on stream water quality and their seasonal changes. *Water Res.* **2021**, *191*, 116811. [CrossRef] [PubMed]
48. Dunea, D.; Bretcan, P.; Tanislav, D.; Serban, G.; Teodorescu, R.; Iordache, S.; Petre, B.; Tuchiu, E. Evaluation of Water Quality in Ialomita River Basin in Relationship with Land Cover Patterns. *Water* **2020**, *12*, 735. [CrossRef]
49. Lei, C.; Wagner, P.D.; Fohrer, N. Effects of land cover, topography, and soil on stream water quality at multiple spatial and seasonal scales in a German lowland catchment. *Ecol. Indic.* **2021**, *120*, 106940. [CrossRef]
50. Liu, X.; Zhang, Y.; Li, Z.; Li, P.; Xu, G.; Cheng, Y.; Zhang, T. Response of water quality to land use in hydrologic response unit and riparian buffer along the Dan River, China. *Environ. Sci. Pollut. Res.* **2021**, *28*, 28251–28262. [CrossRef]
51. Song, Y.; Song, X.; Shao, G.; Hu, T. Effects of Land Use on Stream Water Quality in the Rapidly Urbanized Areas: A Multiscale Analysis. *Water* **2020**, *12*, 1123. [CrossRef]
52. Gu, Q.; Hu, H.; Ma, L.; Sheng, L.; Yang, S.; Zhang, X.; Zhang, M.; Zheng, K.; Chen, L. Characterizing the spatial variations of the relationship between land use and surface water quality using self-organizing map approach. *Ecol. Indic.* **2019**, *102*, 633–643. [CrossRef]
53. Zhou, P.; Huang, J.; Robert, R.G., Jr.; Hong, H. New insight into the correlations between land use and water quality in a coastal watershed of China: Does point source pollution weaken it? *Sci. Total. Environ.* **2016**, *543*, 291–600. [CrossRef] [PubMed]